Synthesis and characterization of lead-free $0.5Ba(Zr_{0.2}Ti_{0.8})O_3$-$0.5(Ba_{0.7}Ca_{0.3})TiO_3$ ceramic

Indrani Coondoo' , Neeraj Panwar, Harvey Amorín, Miguel Alguero, and A. L. Kholkin

Citation: Journal of Applied Physics **113**, 214107 (2013); doi: 10.1063/1.4808338
View online: http://dx.doi.org/10.1063/1.4808338
View Table of Contents: http://aip.scitation.org/toc/jap/113/21
Published by the American Institute of Physics

Synthesis and characterization of lead-free $0.5Ba(Zr_{0.2}Ti_{0.8})O_3$-$0.5(Ba_{0.7}Ca_{0.3})TiO_3$ ceramic

Indrani Coondoo,[1,a)] Neeraj Panwar,[1] Harvey Amorín,[2] Miguel Alguero,[2] and A. L. Kholkin[1]
[1]*Department of Materials and Ceramics Engineering & CICECO, University of Aveiro, 3810 193 Aveiro, Portugal*
[2]*Instituto de Ciencia de Materiales de Madrid, CSIC, Cantoblanco, 28049 Madrid, Spain*

(Received 2 April 2013; accepted 16 May 2013; published online 5 June 2013)

Polycrystalline sample of lead-free $0.5Ba(Zr_{0.2}Ti_{0.8})O_3$-$0.5(Ba_{0.7}Ca_{0.3})TiO_3$ ceramic has been synthesized by solid state reaction method. Single-phase perovskite structure with rhombohedral symmetry was confirmed by x-ray diffraction. Temperature dependent dielectric permittivity studies demonstrated frequency independent behavior, indicating that the studied sample was not a typical relaxor ferroelectric. A polymorphic phase transition between rhombohedral and tetragonal phase was noticed near room temperature followed by a tetragonal to cubic transition with 97 °C as the temperature of maximum permittivity. The macroscopic values of d_{33} and d_{31} were ~350 pC/N and −141 pm/V, whereas the electromechanical coupling factors k_p and k_t were 44.5% and 41.6%, respectively. Bulk P-E hysteresis loop was obtained with saturation polarization 11 $\mu C/cm^2$ and coercive field ~4 kV/cm. Distinct polarization contrast with a complex mosaic-like domain structure was observed in the *out-of-plane* mode of piezoresponse force microscopy. The domain width and the correlation length were estimated to be nearly 2 μm and 827 nm, respectively. Local hysteresis loop with apparent coercive voltage, $V_c = 15.8$ V, was observed. © *2013 AIP Publishing LLC*. [http://dx.doi.org/10.1063/1.4808338]

I. INTRODUCTION

So far, lead zirconate titanates (PZT) were the most widely used piezoelectric materials due to their excellent piezoelectric properties in the vicinity of the morphotropic phase boundary (MPB) between rhombohedral and tetragonal phases.[1] However, with the recent growing demands for the environmental protection from elements like lead (Pb), there is worldwide focus on the search of lead-free materials with electromechanical properties comparable to PZT.[2–5] In this regard, several lead-free systems have emerged out including $(Na_{0.5}K_{0.5})NbO_3$ (NKN), ZnO, $(Bi_{0.5}Na_{0.5})TiO_3$ (BNT), and $BaTiO_3$ (BT) based compositions.[2,6–10] Although the piezoelectric coefficient values of NKN and BNT systems have been improved using site engineering,[11–13] sintering aid[14] or a new synthesis technique;[2] their main drawbacks include the presence of highly volatile elements like Bi, Na, and K. This results in poor densification that leads to degradation in the physical properties. Moreover, the hygroscopic nature of these systems further hinders their applications. As far as BT is concerned, astonishingly high d_{33} values of 350 460 pC/N have been reported in ceramics prepared by microwave sintering, ordinary sintering, and two-step sintering processes.[15–17] Additionally, BT does not possess any volatile elements and its properties can be easily tailored by site engineering. The solid solution of BT and barium zirconate ($BaZrO_3$), $Ba(Zr_yTi_{1-y})O_3$ (BZT) was considered as an important material for the fabrication of ceramic capacitors because Zr^{4+} is chemically more stable than Ti^{4+}.[18,19] The related system $(Ba_{1-x}Ca_x)(Zr_yTi_{1-y})O_3$ (BCZT) ceramics was reported to exhibit dielectric constant values as high as ~18 000.[20] Recently, Liu and Ren optimized the BZT-*x*BCT composition to a triple point and observed a very high d_{33} value ~620 pC/N.[21] BZT-*x*BCT shows a phase diagram similar to the Pb-based systems, with a MPB starting from a triple point of a paraelectric cubic phase, ferroelectric rhombohedral and tetragonal phases.[22] This triple point is shown to be a tricritical point, and thus the system exhibits very high piezoelectric performance. This finding led to a surge of worldwide investigation on BT-based ceramics possessing a good potential of replacing lead-containing PZT materials. For example, Xue *et al.* determined a full set of elastic, dielectric, and piezoelectric constants for the 50BZT-50BCT ceramic by using a resonance method and measured the temperature dependence of electrical properties.[23] Gao *et al.* studied the microstructure evolution around its MPB by transmission electron microscopy (TEM).[24] Su *et al.* investigated the poling dependence and stability of the electrical properties of 50BZT-50BCT ceramics.[25] Zeng *et al.* reported the fabrication of BCT-BZT single crystal.[26] Piorra *et al.* investigated electrical properties of 50BZT-50BCT thin films deposited by pulsed laser deposition technique.[27] Yao *et al.* reported high pyroelectricity (5.84×10^{-4} C m^{-2} K^{-1} at room temperature) in this system.[28] Damjanovic *et al.* reported Raman spectra and temperature induced anomalies in dielectric and elastic coefficients of BCZT.[29] Li *et al.* reported the dielectric properties of BCT-BZT as a function of Ca-doping.[30] Wang *et al.* synthesized BCT-BZT nanoparticles with size ranging from 30 to 60 nm by sol-gel method at relatively low temperature (650 °C).[31] Puli *et al.* demonstrated high dielectric breakdown and excellent energy storage capacity in the BCT-BZT

a)Author to whom correspondence should be addressed. Electronic mail: indrani coondoo@yahoo.com

ceramics.[32] Li *et al*. examined temperature stability of the piezoelectric properties of yttrium doped BCT-BZT system.[33] Similarly, effect of sintering aids and site substitution, especially on the piezoelectric properties, have been carried out in the parent BCZT system recently. Thus, based on the available literature, one can conclude that BCZT system is better than other existing lead-free compositions and its piezoelectric properties are comparable to PZT. Further, it was noticed that only few reports exist in literature about the local piezoelectric properties measurement on BZT ceramics;[34,35] however, to the best of our knowledge, such studies have not been performed so far on the BCZT system by piezoresponse force microscopy (PFM) mode of scanning probe microscopy (SPM) technique. Therefore, the present study focuses on the PFM studies alongwith other bulk properties including morphological, dielectric, ferroelectric, and piezoelectric properties of the BCZT system.

II. EXPERIMENTAL

The $0.5Ba(Zr_{0.2}Ti_{0.8})O_3$-$0.5(Ba_{0.7}Ca_{0.3})TiO_3$ [BCZT] ceramic was prepared by conventional solid-state reaction technique in which stoichiometric ratios of $BaCO_3$ (99.9%), $CaCO_3$ (99%), TiO_2 (99%), and ZrO_2(99%) were mixed. Calcination was performed at 1200 °C for 6 h. The calcined powder was then pressed into pellets (using polyvinyl alcohol as a binder) and sintered at 1450 °C for 2 h in air. Phase formation was confirmed by x-ray diffractometer (XRD, Phillips X'pert). The microstructure was obtained using Scanning Electron Microscope (SEM) Hitachi S4100 at 25 kV. For electrical characterization, silver paste was painted on both circular surfaces of the sample and cured at 600 °C for 30 min. The dielectric constant and loss tangent as a function of temperature and frequency were measured using a HP 4284A precision LCR meter. Polarization-electric field hysteresis loops were obtained by current integration. Voltage sine waves were applied (0.1 Hz) by the combination of a synthesizer/function generator (HP 3325B) and a high voltage amplifier (TREK model 10/40), and charge was measured with a homebuilt charge to voltage converter. Bulk piezoelectric charge coefficient, d_{33} was measured on poled samples by a Berlincourt piezometer (Channel products, Inc., Chesterland, OH). The samples were poled at 80 °C in silicon oil bath by applying a DC electric field of 4.2 kV/mm for 20 min, and field-cooled to room temperature. The transverse piezoelectric coefficient and coupling factors were acquired using complex analysis of piezoelectric radial resonances of the discs by an automatic iterative method. Local piezoelectric properties of the sample were investigated with PFM (simultaneously acquired with topography) using NT-MDT commercial setup equipped with a lock-in amplifier (SR-830A, Stanford Research) and a function generator (FG-120, Yokagawa). Platinum coated silicon cantilever (force constant 42 N/m and resonance frequency 204 497 kHz) was used for this study. PFM images were obtained by applying ac voltage (5 V, peak-to-peak) with frequency of 50 kHz between the grounded tip and the bottom electrode. Switching spectroscopy PFM (SS-PFM) in the so-called pulse mode was used to obtain local hysteresis curves that consists of applying dc voltages, V_{dc}, for a short time (0.5 s). PFM signal (proportional to the d_{33}) was measured between the increasing voltage pulses (period ~2 s) with steps of 0.1 V. AC voltage (10 V peak-to-peak) and frequency of 50 kHz were used for loop acquisition.

III. RESULTS AND DISCUSSION

Figure 1 presents the XRD pattern of the sintered BCZT ceramic. The sample exhibits perovskite structure with no trace of impurity, suggesting that Ca and Zr diffuse into the $BaTiO_3$ lattice to form a homogeneous solid solution. A single peak at $2\theta = 45°$ alongwith the splitting of the 66° diffraction peak into (220)/(202) indicates the perovskite structure to be rhombohedral (inset of Fig. 1). Figure 2(a) shows the scanning electron micrograph of the as-sintered ceramic sample. Well connected grains separated by grain boundaries can be noticed. The grains are of varying size with average size ~25 μm, which is much larger than the average grain size (3 5 μm) of other known lead-free compositions like (Bi,Na)TiO_3 and (K,Na)NbO_3. Energy Dispersive Spectrometry (EDAX) measurement (Figure 2(b)) shows all the elemental peaks of BCZT sample.

Figure 3(a) shows the temperature dependent dielectric permittivity of BCZT sample at various frequencies ranging from 100 Hz to 1 MHz. The dielectric permittivity value ~2600 at room temperature is consistent with earlier reports.[28,30,33] It is also observed that the permittivity exhibits a frequency independent behavior, indicating that the studied sample is not a typical relaxor ferroelectric. Moreover, a polymorphic phase transition (PPT) between rhombohedral and tetragonal phase takes place near room temperature (indicated by an arrow) followed by a tetragonal to cubic transition with 97 °C as the temperature of maximum permittivity (T_m). The T_m is higher than many previously reported data[12] but lower than in Refs. 2 and 30. Additionally, it is observed that the higher temperature phase transition region is broad, with full width of half maximum (FWHM) extending to about 40 °C, suggesting a diffused

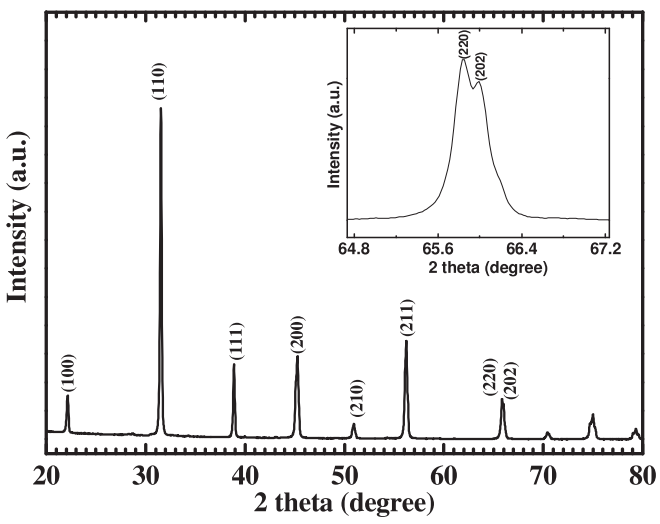

FIG. 1. X ray diffraction pattern of BCZT ceramic sample. The inset is enlarged view of the diffraction peak at 66°.

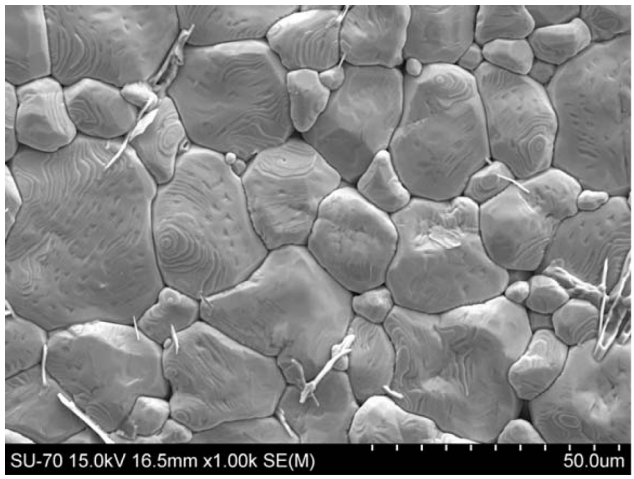

(a)

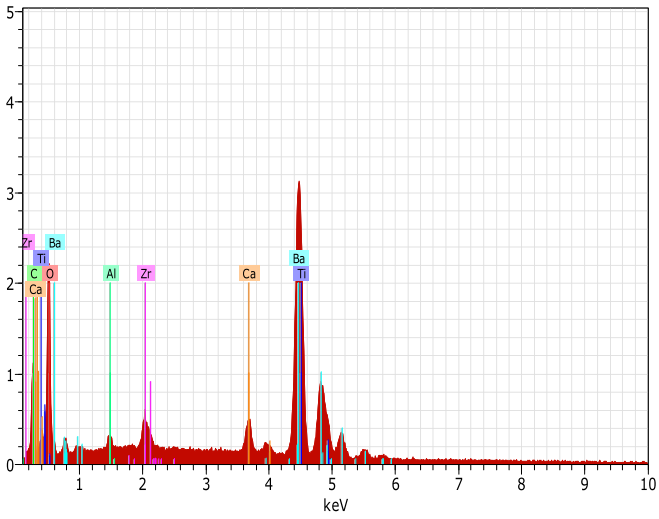

(b)

FIG. 2. (a) SEM micrograph and (b) EDAX pattern of BCZT sample.

phase transition (DPT) in this material. The dielectric dispersion in case of a DPT can be determined from the empirical relation:[36]

$$\left(\frac{1}{\varepsilon}-\frac{1}{\varepsilon_m}\right)=\frac{(T-T_m)^{\gamma}}{C}, \tag{1}$$

where ε_m is the dielectric constant maximum at T_m while γ and C are constants. Two quantitative parameters of relative broadness (or diffuseness) in the dielectric spectra are the diffuseness exponent (γ) and the degree of diffuseness (δ). The diffuseness exponent can vary from 1, for a normal ferroelectric, to 2 for an ideal relaxor ferroelectric. The logarithmic form of Eq. (1) would take the following form:

$$\ln\left(\frac{1}{\varepsilon}-\frac{1}{\varepsilon_m}\right)=\gamma\ln(T-T_m)+\ln C. \tag{2}$$

Inset of Figure 3(a) shows the linear graph between ln ($1/\varepsilon - 1/\varepsilon_m$) and ln ($T$-$T_m$). A low $\gamma \sim 1.59$ alongwith the degree of relaxation parameter ΔT_m ($=T_{m(1\text{kHz})}-T_{m(1\text{MHz})}$) value equal to zero suggests that the studied material is nonrelaxor. The parameter δ which is related with permittivity as follows:[37]

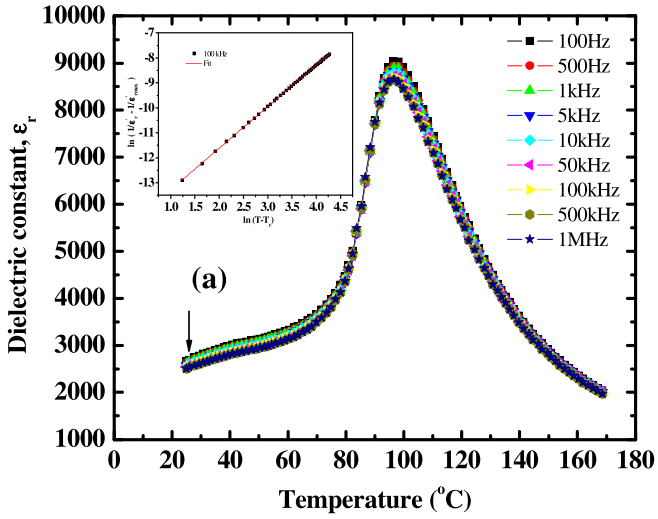

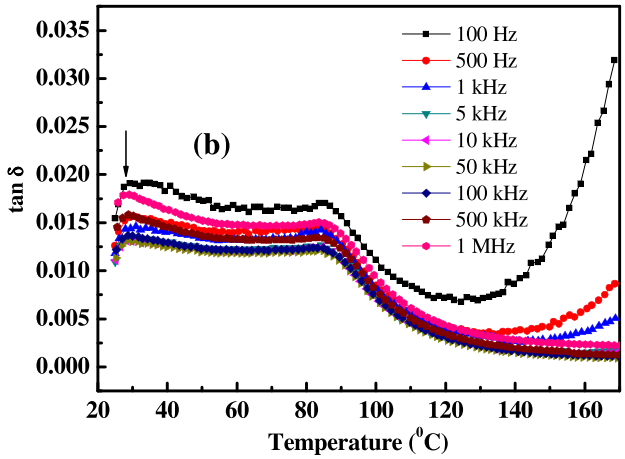

FIG. 3. (a) Dielectric constant and (b) tangent loss as a function of measuring temperature and frequency of BCZT sample. Inset in (a) shows the fitting with Eq. (2).

$$C=2\varepsilon_m\delta^{\gamma} \tag{3}$$

possesses a value ~11 °C. The frequency independent broadened dielectric maximum and its deviation from Curie-Weiss law are the main characteristics of a DPT in the studied material. Similar observation has also been reported in $BaTi_{1-x}Sn_xO_3$ with $x < 15\%$ assigned to the nonrelaxor DPT-ferroelectric characteristics.[38,39] The broadness or diffusiveness in such materials occurs mainly due to the compositional fluctuation and/or structural disordering in the arrangement of cation(s) in one or more crystallographic sites causing a microscopic heterogeneity in the compound with different local Curie points. Besides compositional fluctuation, mechanical stress in the grain (generally introduced in the lattice during post sintering cooling, wherein a transition from cubic to tetragonal phase occurs below T_m) also plays a role in diffuseness of the permittivity near T_m.[40] In the studied composition, Ba^{2+} (1.35 Å) and Ca^{2+} (0.99 Å) ions enter the A site of the ABO_3 perovskite structure, whereas Zr^{4+} (0.98 Å) and Ti^{4+} (0.72 Å) ions occupy the B site. Krishna *et al.* have reported the probability of Ca^{2+} ion occupying the Ti^{4+} site in the $BaTiO_3$ lattice leading to a compositional disorder.[41] Also, it has been reported that at higher Zr contents (>0.08), BCZT ceramic shows a broadened permittivity behavior near

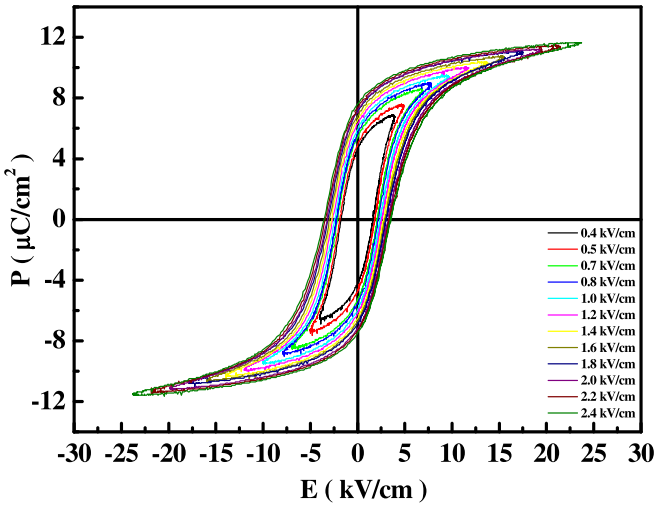

FIG. 4. Macroscopic polarization versus electric field hysteresis loop.

T_m, caused by compositional fluctuation. The effect of internal stresses in the present case is negligible because of the larger grain size.

Figure 3(b) shows the tangent loss as a function of temperature at various frequency values. There are two peaks observed in the loss versus temperature ($\tan\delta$-T) graph. The anomaly near room temperature depicts the PPT between rhombohedral and tetragonal phase (prominently visible in this case as compared to ε_r-T curve). The loss at higher temperatures shows a frequency dependent dispersion and its higher value indicates space charge polarization and associated ionic conductivity. Nevertheless, the maximum value of the dielectric loss remains <0.32.

Figure 4 displays polarization versus electric field (P-E) loops of the BCZT sample acquired at room temperature in the electric field ranging from 0.4 to 2.4 kV/cm. The material exhibits classical ferroelectric-like loops. The remnant polarization (P_r) and coercive field (E_c) values are 8 μC/cm^2 and ~4 kV/cm, respectively, which match well with the published data. Such a low coercive field implies that the BCZT ceramic is "soft" with respect to the electric field. Further, the piezoelectric coefficients d_{33} and d_{31} are ~350 pC/N and −141 pm/V while the electromechanical coupling factors k_p and k_t are 44.5% and 41.6%, respectively. These values are comparable with the reported data on this material.[42]

Domain structures of the ceramics have been studied by PFM. Domain imaging of ferroelectric materials by PFM technique is advantageous over other conventional methods due to the ultrahigh resolution (down to a few nanometers) and the capability of local poling through the PFM-tip bias. Figure 5(a) shows the surface topography of the polished BCZT sample having an average root mean square roughness 2.83 nm. The representative *out-of-plane-polarization* (OPP) PFM amplitude and phase images are shown in Figures 5(b) and 5(c), respectively. The PFM image was taken on an area = 10 × 10 μm^2, lying well within a single grain and is characterized by domain-like polar structure having distinct contrast between bright and dark areas indicating significant out-of-plane component of polarization. At the same time, a large fraction of grey regions (exhibiting weak piezosignal) were observed corresponding to domains with the polarization vector at an angle to the surface.[43] A complex mosaiclike domain structure is revealed with domain width approximately 2 μm as determined from the cross profile across line AB in piezoresponse image (Fig. 5(d)). The autocorrelation function has also been used for the estimation of average domain size. Figure 5(e) shows the three-dimensional auto-correlation image obtained using transformation of

$$C(r_1, r_2) = \sum_{x,y} D(x, y) * D(x + r_1, y + r_2), \tag{4}$$

where $D(x, y)$ is the phase signal at a point in the PFM image and $D(x + r_1, y + r_2)$ is the signal at a point translated by (r_1, r_2). The peak in Figure 5(e) corresponds to the average size of the areas with uniform polarization direction. The behavior of the average auto-correlation function is shown in Figure 5(f), fitted with the formula[44]

$$C(R)\alpha e^{(-(R/R_C))^{2h}}, \tag{5}$$

where R is the radius, R_C is the correlation length, and h is a parameter ($0 < h < 1$). The best fit yields values of the correlation length $R_C = 827$ nm with the exponent value $h = 0.84$. The average domain size is approximately twice the correlation length.

In the present case, the domain morphology does not possess a preferred crystallographic orientation. This is typical of polycrystalline ferroelectric ceramics wherein the domain structure is far more complicated than single crystals, owing to the distribution of permittivity and polarization axes, the elastic and dielectric boundary conditions of the grains, and the internal properties of grain boundaries.[45] Moreover, since the sample in the present study possesses rhombohedral structure at room temperature, eight different values of the vertical piezoresponse signal is expected for arbitrarily oriented grains.[38] This accounts for the complexity of the contrast distribution in the obtained image rendering it difficult to relate these directions to definite crystallographic axes. The large domain size alongwith the absence of labyrinth-type domain pattern indicates the nonexistence of relaxor characteristics, corroborating the bulk dielectric studies. In order to quantify the piezoresponse contrast, piezohistogram, which represents statistical distribution of the measured piezoelectric signal by a number of pixels corresponding to a certain signal level, was studied (Fig. 5(g)). The maximum in piezo-distribution corresponds to the most probable domain configurations and its width reflects the number of available domain states. The curve can be deconvoluted into two peaks lying on either side of the zero piezoresponse with the measured response centered at −51.7 mV for "negative" and at +55.6 mV for "positive" domains. Tip-induced poling (−8 V dc voltage) inside a well-defined area of 6 × 6 μm^2 results in the formation of localized domain with well-saturated polarization as shown in Figure 5(h). The cross-section of the piezoresponse (inset of Fig. 5(h)) along line AB indicates that polarization is uniform inside the poled region.

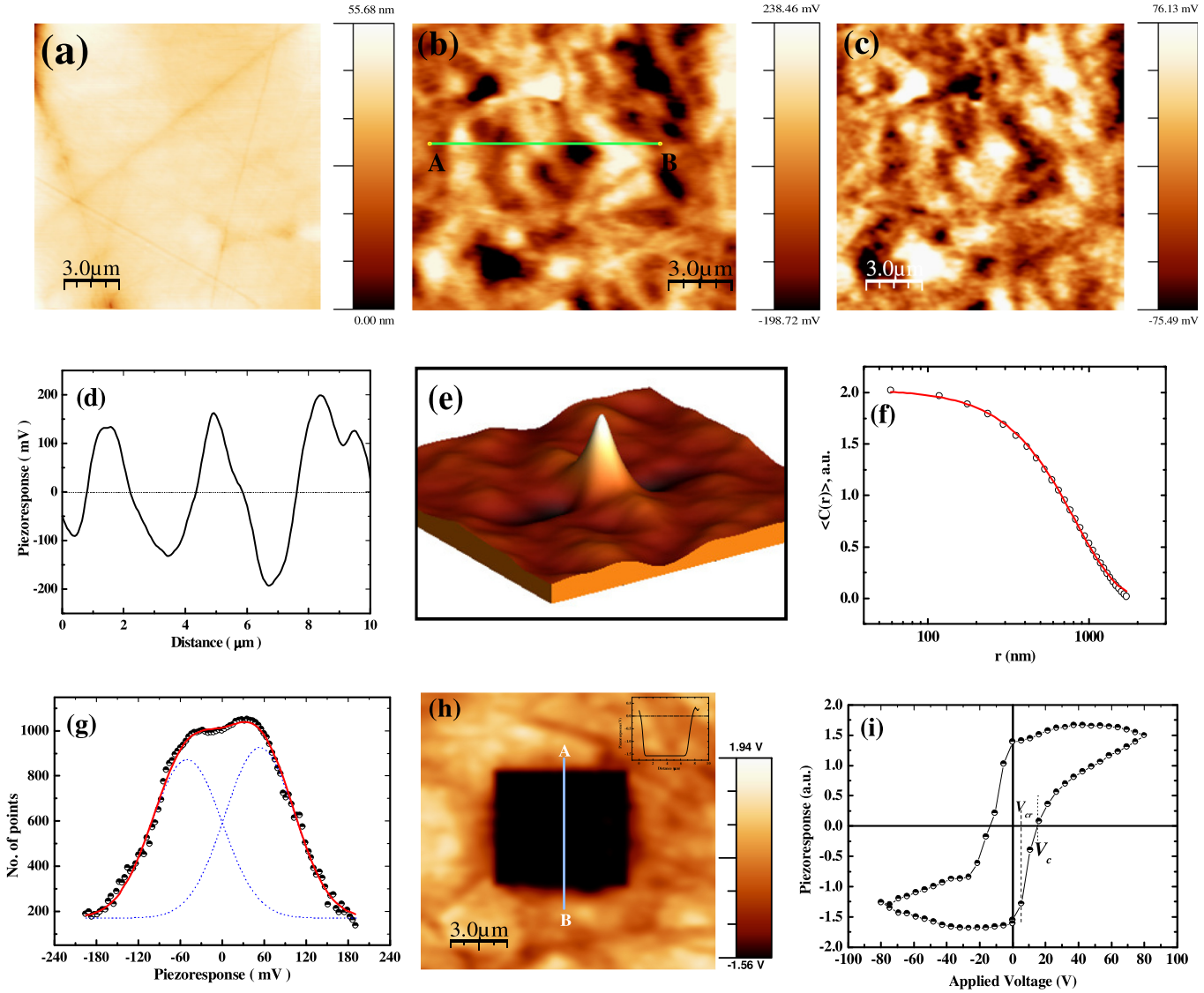

FIG. 5. (a) Topography; (b) OPP PFM amplitude; (c) OPP PFM phase; (d) cross profile along AB in b; (e) 3D auto correlation image of the PFM phase data (scale is arbitrary along the vertical axis); (f) Distance dependence of the auto correlation function $\langle C(r)\rangle$ averaged over all directions corresponding to the 3D auto correlation image in e. Red line represents the best fit; (g) histogram OPP image; (h) square pattern writing (inset is the cross section piezoresponse across line AB); and (i) local piezo hysteresis loop of the BCZT sample.

To compare the bulk and the surface behavior, switchable piezoelectric hysteresis loop was studied by PFM as well. In case of local hysteresis loop, switching occurs in the strongly inhomogeneous electric field below the tip inside individual or a few neighboring domains.[46] This is in contrast to acquiring macroscopic loop with a collective effect of domain nucleation and domain wall motion occurring in an ensemble of grains. Typical local piezoloop measured at room temperature on a fixed location in the center of the BCZT grain is shown in Figure 5(i) which exhibits a tilted loop. The measurements were done in a dc voltage range $-80\,\text{V} \leq V_{\text{dc}} \leq 80\,\text{V}$ that correspond to a very high local electric field concentrated under the tip. The slope of the piezoresponse near the coercive field was about 4.6. The estimated values of critical voltage, V_{cr}, (defined as the voltage necessary to nucleate a new domain where the piezoresponse value starts to change abruptly) and the apparent coercive voltage, V_c, from the local hysteresis loop, were found to be 5.33 and 15.8 V, respectively. It can be noticed that the coercive voltage for the local piezoelectric effect (V_c) is much lower than that required for the macroscopic hysteresis loop. Further, the local piezoloop is not well saturated which is an indication of incomplete and unstable switched state within the time scale of loop acquisition or can be attributed to an increased electrostatic contribution at high bias. Moreover, the switching is quite symmetric without any imprint behavior as there is no difference between positive and negative coercive voltages.

IV. CONCLUSIONS

$0.5Ba(Zr_{0.2}Ti_{0.8})O_3$-$0.5(Ba_{0.7}Ca_{0.3})TiO_3$ lead free ceramic sample has been synthesized following solid state reaction route with 1450 °C as the sintering temperature. The sample possesses single phase rhombohedral structure at room temperature. The bulk d_{33} value of the poled sample is 350 pC/N with high electromechanical coupling factors k_p (44.5%) and k_t (41.6%). The Curie temperature of the sample

as determined from the dielectric versus temperature behavior is ~97 °C. Ferroelectric P-E hysteresis loop was obtained with remnant polarization 8 $\mu C/cm^2$ and coercive field 4 kV/cm. Further, piezoresponse mode of the scanning probe microscopy technique was utilized to investigate the local piezoelectric properties. Distinct polarization contrast was observed in *out-of-plane* mode. A complex mosaiclike domain structure was revealed with domain width ~2 μm and correlation length 827 nm. Local hysteresis loop with apparent coercive voltage, V_c, was found to be 15.8 V.

ACKNOWLEDGMENTS

The authors I.C. and N.P. would like to thank the Portuguese Foundation for Science and Technology (FCT) for the Postdoctoral grants through Project Nos. SFRH/BPD/81032/2011 and SFRH/BPD/71289/2010, respectively. Financial support by Spanish MICINN Project MAT2011-23709 is also acknowledged.

[1]G. H. Haertling, J. Am. Ceram. Soc. **82**, 797 (1999).
[2]Y. Saito, H. Takao, T. Tani, T. Nonoyama, K. Takatori, T. Homma, T. Nagaya, and M. Nakamura, Nature **432**, 84 (2004).
[3]J. Rodel, W. Jo, K. T. P. Seifert, E. Anton, and T. Granzow, J. Am. Ceram. Soc. **92**, 1153 (2009).
[4]D. Q. Xiao, J. G. Wu, L. Wu, J. G. Zhu, P. Yu, D. M. Lin, Y. W. Liao, and Y. Sun, J. Mater. Sci. **44**, 5408 (2009).
[5]J. G. Wu, Y. Y. Wang, D. Q. Xiao, and J. G. Zhu, Appl. Phys. Lett. **91**, 132914 (2007).
[6]M. E. Rogers, C. M. Fancher, and J. E. Blendell, J. Appl. Phys. **112**, 052014 (2012).
[7]D. Y. Wang, N. Y. Chan, S. Li, S. H. Choy, H. Y. Tian, and H. L. W. Chan, Appl. Phys. Lett. **97**, 212901 (2010).
[8]K. I. Park, S. Xu, Y. Liu, G. T. Hwang, S. J. L. Kang, Z. L. Wang, and K. J. Lee, Nano Lett. **10**, 4939 (2010).
[9]Y. C. Yang, C. Song, X. H. Wang, F. Zeng, and F. Pan, Appl. Phys. Lett. **92**, 012907 (2008).
[10]D. M. Lin, D. Q. Xiao, J. G. Zhu, and P. Yu, Appl. Phys. Lett. **88**, 062901 (2006).
[11]S. J. Zhang, R. Xia, and T. R. Shrout, Appl. Phys. Lett. **91**, 132913 (2007).
[12]J. G. Wu, D. Q. Xiao, Y. Y. Wang, W. J. Wu, B. Zhang, J. Li, and J. G. Zhu, Scr. Mater. **59**, 750 (2008).
[13]C. Peng, J. F. Li, and W. Gong, Mater. Lett. **59**, 1576 (2005).
[14]C. W. Ahn, H. C. Song, S. Nahm, S. Priya, S. H. Park, K. Uchino, H. G. Lee, and H. J. Lee, J. Am. Ceram. Soc. **89**, 921 (2006).
[15]H. Takahashi, Y. Numamoto, J. Tani, and S. Tsurekawa, Jpn. J. Appl. Phys., Part 1 **45**, 7405 (2006).
[16]S. F. Shao, J. L. Zhang, Z. Zhang, P. Zheng, M. L. Zhao, J. C. Li, and C. L. Wang, J. Phys. D: Appl. Phys. **41**, 125408 (2008).
[17]T. Karaki, K. Yan, T. Miyamoto, and M. Adachi, Jpn. J. Appl. Phys., Part 2 **46**, L97 (2007).
[18]Y. Zhi, A. Chen, R. Guo, and A. S. Bhalla, J. Appl. Phys. **92**, 2655 (2002).
[19]X. G. Tang, K. H. Chew, and H. L. W. Chan, Acta Mater. **52**, 5177 (2004).
[20]P. Hansen, D. Henning, and H. Schreinemacher, J. Am. Ceram. Soc. **81**, 1369 (1998).
[21]W. F. Liu and X. B. Ren, Phys. Rev. Lett. **103**, 257602 (2009).
[22]H. X. Bao, C. Zhou, D. H. Xue, J. H. Gao, and X. B. Ren, J. Phys. D: Appl. Phys. **43**, 465401 (2010).
[23]D. Xue, Y. Zhou, H. Bao, C. Zhou, J. Gao, and X. Ren, J. Appl. Phys. **109**, 054110 (2011).
[24]J. Gao, D. Xue, Y. Wang, D. Wang, L. Zhang, H. Wu, S. Guo, H. Bao, C. Zhou, W. Liu, S. Hou, G. Xiao, and X. Ren, Appl. Phys. Lett. **99**, 092901 (2011).
[25]S. Su, R. Zuo, S. Lu, Z. Xu, X. Wang, and L. Li, Curr. Appl. Phys. **11**, S120 (2011).
[26]Y. Zeng, Y. Zheng, X. Tu, Z. Lu, and E. Shi, J. Crys. Growth **343**, 17 (2012).
[27]A. Piorra, A. Petraru, H. Kohlstedt, M. Wuttig, and E. Quandt, J. Appl. Phys. **109**, 104101 (2011).
[28]S. Yao, W. Ren, H. Ji, X. Wu, P. Shi, D. Xue, X. Ren, and Z. G. Ye, J. Phys. D: Appl. Phys. **45**, 195301 (2012).
[29]D. Damjanovic, A. Biancoli, L. Batooli, A. Vahabzadeh, and J. Trodahl, Appl. Phys. Lett. **100**, 192907 (2012).
[30]W. Li, Z. Xu, R. Chu, P. Fu, and G. Zang, Curr. Appl. Phys. **12**, 748 (2012).
[31]M. Wang, R. Zuo, S. Qi, and L. Liu, J. Mater. Sci.: Mater. Electron. **23**, 753 (2012).
[32]V. S. Puli, A. Kumar, D. B. Chrisey, M. Tomozawa, J. F. Scott, and R. S. Katiyar, J. Phys. D: Appl. Phys. **44**, 395403 (2011).
[33]W. Li, J. Hao, W. Bai, Z. Xu, R. Chu, and J. Zhai, J. Alloys Compd. **531**, 46 (2012).
[34]F. Moura, A. Z. Simoes, C. S. Riccardi, M. A. Zaghete, J. A. Varela, and E. Longo, Process. Appl. Ceram. **5**, 139 (2011).
[35]D. Ricinschi, C. E. Ciomaga, L. Mitoseriu, V. Buscaglia, and M. Okuyama, J. Eur. Ceram. Soc. **30**, 237 (2010).
[36]K. Uchino and S. Nomura, Integr. Ferrolectr. **44**, 55 (1982).
[37]V. V. Kirillov and V. A. Isupov, Ferroelectrics **5**, 3 (1973).
[38]V. V. Shvartsman, W. Kleemann, J. Dec, Z. K. Xu, and S. G. Lu, J. Appl. Phys. **99**, 124111 (2006).
[39]V. Mueller, H. Beige, and H. P. Abicht, Appl. Phys. Lett. **84**, 1341 (2004).
[40]D. Hennings, A. Schnell, and G. Simon, J. Am. Ceram. Soc. **65**, 539 (1982).
[41]P. S. R. Krishna, D. Pandey, V. S. Tiwari, R. Chakravarthy, and B. A. Dasannacharya, Appl. Phys. Lett. **62**, 231 (1993).
[42]J. Wua, D. Xiao, B. Wu, W. Wu, J. Zhu, Z. Yang, and J. Wang, Mater. Res. Bull. **47**, 1281 (2012)
[43]N. Panwar, I. Coondoo, A. Tomar, A. L. Kholkin, V. S. Puli, and R. S. Katiyar, Mater. Res. Bull. **47**, 4240 (2012).
[44]P. Sharma, T. Reece, D. Wu, V. M. Fridkin, S. Ducharme, and A. Gruverman, J. Phys.: Condens. Matter **21**, 485902 (2009).
[45]J. H. Cho, N. R. Yeom, S. J. Kwon, Y. J. Lee, Y. H. Jeong, M. P. Chun, J. H. Nam, J. H. Paik, and B. I. Kim, J. Appl. Phys. **112**, 052005 (2012).
[46]A. N. Morozovska, S. V. Kalinin, E. A. Eliseev, and S. V. Svechnikov, Ferroelectrics **354**, 198 (2007).